GSA DATA REPOSITORY 2019149 Richardson et al.

SUPPLEMENTAL INFORMATION

TECHNIQUES FOR ESTIMATING *D*

Numerous techniques have been developed to estimate *D*. We present a short summary of the techniques used to obtain the estimates of *D* included in the data compilation.

Scarp Modeling

The first estimates of *D* were made by modeling the evolution of fault scarps and paleo-shorelines of known ages (Nash, 1980b; Colman and Watson, 1983; Hanks et al., 1984). Multiple scarp modeling techniques have been developed (Colman and Watson, 1983; Hanks and Andrews, 1989; Avouac et al., 1993) and produce differing results (Avouac and Peltzer, 1993) depending on the height of the scarp, assumptions about the initial geometry, and whether linear or nonlinear flux laws are used to estimate *D* (Pelletier et al., 2006). The simplest solution for the evolution of a fault scarp that forms instantaneously and then evolves gradually due to creep is

$$z(x,t) = a * erf\left(\frac{x}{2\sqrt{Dt}}\right) + bx, \qquad \text{(S-1)}$$

where *erf(x,t)* is the error function, *a* is half the initial vertical difference in elevation along the scarp, *b* is the is the pre-existing slope, and *x* is the distance from the center elevation of the scarp. The function is often evaluated at *x*=0 and is where the scarp is predicted to experience the highest slope gradient (Hanks, 2000). More sophisticated numerical approaches have been developed that allow the entire profile of the scarp to be analyzed (Avouac, 1993; Arrowsmith et al., 1998). Pelletier and coworkers (2006) found that methods that incorporate the entire profile of the scarp in addition to uncertainty in the initial scarp angle yield the most accurate results.

Laplacian and Erosion Rate

Roering (2002) estimated *D* for a transient hillslope profile along the Charwell River on the South Island, New Zealand using the hillslope Laplacian and estimated erosion rates along the profile. Others (Roering et al., 2007; Perron et al., 2009; Hurst et al., 2012) have since used the ridgetop Laplacian and catchment-averaged erosion rates to estimate *D* in conjunction with equation (2) so that

$$D = -\frac{\rho_r}{\rho_s}\frac{E}{\nabla^2 z_R}, \qquad \text{(S-2)}$$

where $\nabla^2 z_R$ is the Laplacian at the ridgeline. An important assumption required for this analysis is that the ridgeline is eroding at the same rate as the base level lowering rate *E* (for example, a bounding river channel). However, due to the long response time required for hillslopes to reach steady state and variability in climate through the Quaternary, this assumption is rarely perfectly met (Fernandes and Dietrich, 1997). Hillslopes are typically the last part of a landscape to respond to changes in channel incision rates or regional tectonics (Furbish and Fagherazzi, 2001). Nonetheless, evidence exists that ridgetop Laplacians do record changes in channel incision rates, albeit with a delay (Hurst et al., 2013).

Relief and Erosion Rate

In addition to the ridgetop Laplacian and erosion rate technique, another relationship has been derived that relates *D*, topographic characteristics, and erosion rate. Roering and coworkers (2007) derived an analytical solution relating dimensionless relief (R^*) and dimensionless erosion rate (E^*):

$$R^* = \frac{1}{E^*}\left(\sqrt{1+\left(E^*\right)^2} - \ln\left(\frac{1}{2}\left(1+\sqrt{1+\left(E^*\right)^2}\right)\right) - 1\right), \qquad \text{(S-3)}$$

where $R^*=E^*/4$, $E^* = (-2\nabla^2 z_R L_H)/S_c$, L_H is the mean hillslope length, and S_c is the critical hillslope angle at which downslope sediment fluxes become infinite. Callaghan (2012) used equation (S-3) to modify E^*, yielding

$$E^* = \frac{2E(\rho_r/\rho_s)L_H}{DS_c}, \qquad \text{(S-4)}$$

where *E* is the erosion rate and can be solved for with cosmogenic radionuclide (CRN) analysis. L_H was calculated by dividing the total basin area by twice the length of the channel network extracted from ASTER DEM data gridded to 30 m (Callaghan, 2012). Callaghan (2012) used the Peukar-Douglas algorithm to define channel heads using landscape curvature and verified the results with georeferenced satellite images.

Callaghan (2012) combined equation (S-3) and equation (S-4) to solve for D for a series of sites along a strong climate gradient along the Chilean coast.

Colluvial Flux and Slope

Hughes and coworkers (2009), in a similar fashion to Reneau and coworkers (1989), estimated the mass of dated colluvium in hollows and used colluvial infilling rates to estimate D. Others (West et al., 2014; McKean et al., 1993) have determined sediment flux rates by measuring the increase in soil ^{10}Be concentration with increasing distance downslope of the ridgetop and using a known rate of meteoric 10Be accumulation to calculate soil creep velocity. These sediment flux rates can be used in conjunction with slope gradients and equation (1) to solve for D.

Landscape Evolution Modeling

Others have estimated D using landscape evolution models (LEMs) and generally utilize error-minimization techniques to tune D so that other characteristics of the landscape are reproduced by the LEM (McGuire et al., 2014; Pelletier et al., 2011; Petit et al., 2009). Roering and coworkers (1999) estimated D for a field site in the Oregon Coast Range by picking a value of D that minimized the error between predicted erosion rates using a nonlinear flux law and a long-term erosion rate determined by CRNs.

SUPPLEMENTAL FIGURE CAPTION

Figure DR1. Plots of *D* against AI for *D* estimated with (A) the scarp modeling technique, (B) the Laplacian and erosion rate technique, (C) the relief and erosion rate technique, and (D) the landscape evolution modeling (green circles) and colluvial flux techniques (purple triangles). Best-fit regression lines fit to the log-transformed data and corresponding R^2 values are included in (A)-(C).

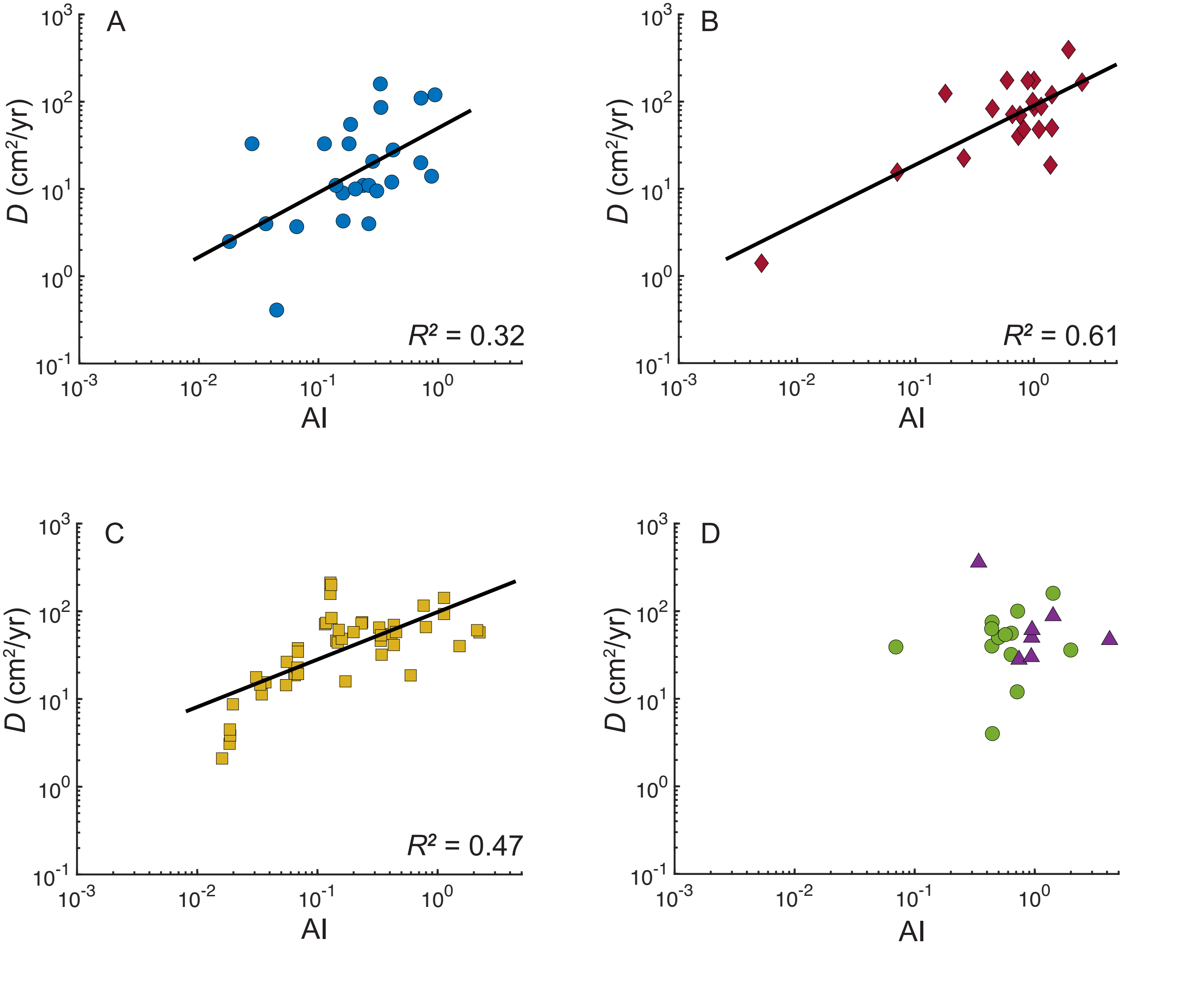

Fig. DR1

SUPPLEMENTAL TABLE CAPTIONS

Table DR1. Compilation of *D* and related data. If multiple estimates of *D* were made at the same site by different studies, we included all of those estimates unless there is evidence that one or more of the estimates is inaccurate. In that case, we excluded the inaccurate estimate(s) from the analysis.

Table DR2. New estimates of *D* made in this study and site information. If more than one erosion rate estimate exists at a site in a suitable location to estimate *D*, we estimated *D* for each erosion rate and assigned the mean of these estimates of *D* as the site *D*. We estimated the uncertainty in *D* as either the standard error of the mean of *D* or the sum in quadrature of the standard errors of individual estimates, whichever is greater. We reported the ridgetop Laplacian of each site as the mean of the unique estimates of the ridgetop Laplacian used to calculate *D* for the site. If there is no published estimate of ρ_r or ρ_s at the site, we use a density ratio of ρ_r/ρ_s = 2 (DiBiase et al., 2010; Heimsath et al., 1999; Hurst, Mudd, Attal, et al., 2013).

SUPPLEMENTAL TABLES

127 **Table DR1**

Source	Site location[a]	Latitude (°)	Longitude (°)	D[b] (cm^2/yr)	AI	MAP (cm/yr)	Underlying lithology description	Lithology category[c]	Technique description	Technique category[d]	Vegetation description	Vegetation category[e]
Almond et al. [2008]	Charwell Basin, New Zealand	-42.450	173.357	50 ± 20	1.42	116	Loess underlain by fluvial gravel terraces	1	Erosion rate and curvature. Estimate is for the Holocene. Similar technique to Roering et al. (2002).	2	Podocarp, hardwood, and beech forest	3
Almond et al. [2008]	Ahuriri, New Zealand	-43.702	172.584	70 ± 20	0.76	68.8	Thick loess deposits underlain by altered basalt	1	^{137}Cs fallout nuclides (50 yr timescale) and curvature. Similar technique to Roering et al. (2002).	2	Recolonization of forest during Holocene. Recently introduced pasture grasses.	2
Arrowsmith et al. (1998)	Carrizo Plain, CA, USA	35.271	-119.827	86 ± 8	0.33	46.7	Conglomerate and alluvial fan units.	2	Scarp modeling	1	Grasses and shrubs	2
Avouac and Peltzer (1993)	Hotan Region, Xinjiang, China	36.800	80.500	33 ± 14	0.03	3.3	Loose fan gravels	1	Scarp modeling	1	Unvegetated	1
Avouac et al. (1993)	Tien Shan, China	44.048	86.790	55 ± 25	0.19	18.4	Loose fan gravels	1	Scarp modeling	1	Grasses and shrubs	2
Begin (1992)	Northern Negev, Israel	31.262	34.802	4 ± 3	0.16	23.3	Fluvial gravel terraces	1	Scarp modeling	1	Unvegetated	1
Ben-Asher et al. (2017)	Odem cinder cone, Golan Heights, Israel	33.197	35.755	12	0.714	79.1	Cinder	1	Assumed initial shape and age in conjunction with a numerical model	3	scrubland	2
Ben-Asher et al. (2017)	Baron cinder cone, Golan Heights, Israel	33.158	35.779	32	0.635	73	Cinder	1	Assumed initial shape and age in conjunction with a numerical model	3	scrubland	2
Ben-Asher et al. (2017)	Bental cinder cone, Golan Heights, Israel	33.130	35.783	56	0.638	72.8	Cinder	1	Assumed initial shape and age in conjunction with a numerical model	3	scrubland	2
Ben-Asher et al. (2017)	Shifon cinder cone, Golan Heights, Israel	33.069	35.771	54	0.569	66.1	Cinder	1	Assumed initial shape and age in conjunction with a numerical model	3	scrubland	2
Ben-Asher et al. (2017)	Fares cinder cones, Golan Heights,	32.960	35.865	63	0.438	53.9	Cinder	1	Assumed initial shape and age in conjunction with a numerical model	3	scrubland	2

	Israel											
Bowman and Gerson (1986)	Lake Lisan, Dead Sea, Israel	31.386	35.361	4	0.07	10.9	Gravel	1	Scarp modeling	1	Unvegetated	1
Bowman and Gross (1989) as reported in Hanks (2000)	Northern Arava, Israel	30.658	35.240	> 4 (4)	0.04	6	Gravel	1	Scarp modeling	1	Unvegetated	1
Callaghan (2012)	Chile	-32.99	-71.42	55 ± 24	0.41	48.2	Granitic	3	Relief and erosion rate	5	Mostly herbaceous with some trees	3
Callaghan (2012)	Chile	-32.98	-71.42	70 ± 36	0.43	51.8	Granitic	3	Relief and erosion rate	5	Mostly herbaceous with some trees	3
Callaghan (2012)	Chile	-32.98	-71.42	41 ± 20	0.43	51.8	Granitic	3	Relief and erosion rate	5	Mostly herbaceous with some trees	3
Callaghan (2012)	Chile	-32.94	-71.43	46 ± 20	0.34	39.7	Granitic	3	Relief and erosion rate	5	Mostly herbaceous with some trees	3
Callaghan (2012)	Chile	-33.01	-71.44	58 ± 27	0.45	53.1	Granitic	3	Relief and erosion rate	5	Herbaceous with few trees	2
Callaghan (2012)	Chile	-31.12	-71.58	46 ± 7	0.14	16.7	Granitic	3	Relief and erosion rate	5	Mostly herbaceous with some trees	3
Callaghan (2012)	Chile	-31.12	-71.56	44 ± 13	0.15	16.7	Granitic	3	Relief and erosion rate	5	Mostly herbaceous with some trees	3
Callaghan (2012)	Chile	-31.12	-71.55	49 ± 13	0.16	18.3	Granitic	3	Relief and erosion rate	5	Mostly herbaceous with few trees with some bare ground	2
Callaghan (2012)	Chile	-30.55	-71.63	158 ± 68	0.13	13.8	Granitic	3	Relief and erosion rate	5	Mostly herbaceous with some trees	3
Callaghan (2012)	Chile	-30.55	-71.63	212 ± 92	0.13	13.8	Granitic	3	Relief and erosion rate	5	Mostly herbaceous with few trees and some bare ground	2
Callaghan (2012)	Chile	-29.62	-71.20	38 ± 13	0.07	7.6	Granitic	3	Relief and erosion rate	5	Mostly herbaceous with few trees and some bare ground	2
Callaghan (2012)	Chile	-29.62	-71.20	38 ± 11	0.07	7.6	Granitic	3	Relief and erosion rate	5	Mostly herbaceous with few trees and some bare ground	2
Callaghan (2012)	Chile	-29.62	-71.20	35 ± 12	0.07	7.6	Granitic	3	Relief and erosion rate	5	Mostly herbaceous with few trees and some bare ground	2
Callaghan (2012)	Chile	-29.58	-71.14	20 ± 7	0.06	7.3	Granitic	3	Relief and erosion rate	5	Mostly herbaceous with few trees and some bare	2

											ground	
Callaghan (2012)	Chile	-29.57	-71.16	19 ± 7	0.06	7.4	Granitic	3	Relief and erosion rate	5	Mostly herbaceous with few trees and some bare ground	2
Callaghan (2012)	Chile	-29.22	-71.18	27 ± 9	0.06	6.5	Granitic	3	Relief and erosion rate	5	Mixture of herbaceous groundcover and bare ground	2
Callaghan (2012)	Chile	-29.23	-71.18	14 ± 5	0.05	6.5	Granitic	3	Relief and erosion rate	5	Mixture of herbaceous groundcover and bare ground	2
Callaghan (2012)	Chile	-28.41	-71.05	16 ± 7	0.04	4.7	Granitic	3	Relief and erosion rate	5	Mostly bare ground with some herbaceous ground cover	1
Callaghan (2012)	Chile	-28.40	-71.06	11 ± 5	0.03	4.5	Granitic	3	Relief and erosion rate	5	Bare ground	1
Callaghan (2012)	Chile	-28.39	-71.07	15 ± 7	0.03	4.3	Granitic	3	Relief and erosion rate	5	Bare ground	1
Callaghan (2012)	Chile	-28.36	-71.05	18 ± 9	0.03	4	Granitic	3	Relief and erosion rate	5	Bare ground	1
Callaghan (2012)	Chile	-26.57	-70.44	2 ± 1	0.02	2	Granitic	3	Relief and erosion rate	5	Bare ground	1
Callaghan (2012)	Chile	-26.56	-70.48	3 ± 1	0.02	2.3	Granitic	3	Relief and erosion rate	5	Bare ground	1
Callaghan (2012)	Chile	-26.56	-70.51	4 ± 2	0.02	2.3	Granitic	3	Relief and erosion rate	5	Bare ground	1
Callaghan (2012)	Chile	-26.59	-70.49	4 ± 2	0.02	2.3	Granitic	3	Relief and erosion rate	5	Bare ground	1
Callaghan (2012)	Chile	-26.57	-70.56	9 ± 4	0.02	2.4	Granitic	3	Relief and erosion rate	5	Bare ground	1
Callaghan (2012)	Chile	-40.58	-73.69	58 ± 17	2.23	184	Granitic	3	Relief and erosion rate	5	Forested	5
Callaghan (2012)	Chile	-40.58	-73.60	61 ± 20	2.13	178	Granitic	3	Relief and erosion rate	5	Forested	5
Callaghan (2012)	Chile	-37.90	-73.28	40 ± 14	1.52	169	Granitic	3	Relief and erosion rate	5	Forested	5
Callaghan (2012)	Chile	-36.97	-73.12	93 ± 45	1.13	123	Granitic	3	Relief and erosion rate	5	Forested	5
Callaghan (2012)	Chile	-36.97	-73.12	142 ± 65	1.13	123	Granitic	3	Relief and erosion rate	5	Forested	5
Callaghan (2012)	Chile	-35.84	-72.51	66 ± 23	0.80	90.7	Granitic	3	Relief and erosion rate	5	Forested	4
Callaghan (2012)	Chile	-35.86	-72.48	116 ± 42	0.76	85.3	Granitic	3	Relief and erosion rate	5	Forested	4
Callaghan (2012)	Chile	-34.61	-71.58	19 ± 12	0.60	75.5	Granitic	3	Relief and erosion rate	5	Mostly herbaceous with few trees	2

Callaghan (2012)	Chile	-33.88	-71.50	65 ± 29	0.33	42.3	Granitic	3	Relief and erosion rate	5	Herbaceous	2
Callaghan (2012)	Chile	-33.90	-71.49	32 ± 14	0.34	45.2	Granitic	3	Relief and erosion rate	5	Herbaceous	2
Callaghan (2012)	Chile	-32.94	-71.42	53 ± 23	0.34	39.6	Granitic	3	Relief and erosion rate	5	Mostly herbaceous with some trees	3
Callaghan (2012)	Chile	-32.27	-71.41	75 ± 31	0.24	30.1	Granitic	3	Relief and erosion rate	5	Mostly herbaceous with some trees	3
Callaghan (2012)	Chile	-32.27	-71.40	73 ± 38	0.23	30	Granitic	3	Relief and erosion rate	5	Mostly herbaceous with some trees	3
Callaghan (2012)	Chile	-32.08	-71.42	58 ± 28	0.20	25.9	Granitic	3	Relief and erosion rate	5	Mostly herbaceous with some trees	3
Callaghan (2012)	Chile	-31.56	-71.42	61 ± 16	0.15	18.8	Granitic	3	Relief and erosion rate	5	Mostly herbaceous	2
Callaghan (2012)	Chile	-31.52	-71.42	16 ± 4	0.17	20.8	Granitic	3	Relief and erosion rate	5	Mostly herbaceous with some trees	3
Callaghan (2012)	Chile	-30.52	-71.66	71 ± 29	0.12	12.6	Granitic	3	Relief and erosion rate	5	Mostly herbaceous with some trees	3
Callaghan (2012)	Chile	-30.53	-71.66	74 ± 30	0.12	13	Granitic	3	Relief and erosion rate	5	Mostly herbaceous with few trees	2
Callaghan (2012)	Chile	-30.55	-71.62	84 ± 37	0.13	14	Granitic	3	Relief and erosion rate	5	Mostly herbaceous with some trees	3
Callaghan (2012)	Chile	-30.57	-71.63	200 ± 88	0.13	14	Granitic	3	Relief and erosion rate	5	Mostly herbaceous with few trees	2
Callaghan (2012)	Chile	-29.65	-71.11	23 ± 8	0.07	7.5	Granitic	3	Relief and erosion rate	5	Mostly bare ground	1
Callaghan (2012)	Chile	-29.67	-71.16	19 ± 7	0.07	7.7	Granitic	3	Relief and erosion rate	5	Mixture of herbaceous groundcover and bare ground	2
Carretier et al. (2002)	Gurvan Bugd fault system, Mongolia	44.840	100.303	33 ± 17	0.18	13.9	Gravel	1	Scarp modeling	1	Unvegetated	1
Colman and Watson (1983)	Lane Bonneville, UT, USA	39.625	-113.211	9	0.16	19.9	Gravel	1	Scarp modeling	1	Grasses and shrubs	2
Enzel et al. (1996)	Southern Arava Valley, Israel	29.612	34.983	2-3 (2.5)	0.02	3.1	Sandy gravel	1	Scarp modeling	1	Unvegetated	1
Hanks (2000)	Lost River, ID, USA	44.166	-113.870	9-10 (9.5)	0.31	28.3	Alluvial gravel	1	Scarp modeling	1	Sagebrush and grasses	2
Hanks and Wallace (1985)	Lake Lahonta, NV, USA	40.152	-117.925	11	0.14	18.8	Alluvial deposits	1	Scarp modeling	1	Some vegetation	2

Hanks et al. (1984)	Lake Bonneville, UT, USA	39.613	-112.299	11	0.24	29.5	Gravels	1	Scarp modeling	1	Grasses and shrubs	2
Hanks et al. (1984)	Santa Cruz sea cliffs, CA, USA	36.984	-122.127	110	0.72	79.8	Mudstone	2	Scarp modeling	1	The lower terraces are farmed while the upper terraces are covered with grasslands. The lower terraces have never been forested (Rosenbloom & Anderson, 1994).	2
Hanks et al. (1984)	Raymond Fault Scarp, LA, CA, USA	34.119	-118.131	160	0.33	46.2	Coarse alluvial deposits	1	Scarp modeling	1	Grasses and some trees	3
Hanks et al. (1984)	Drum Mtnts., UT, USA	39.650	-112.136	11	0.26	32.6	Alluvial gravels	1	Scarp modeling	1	Low shrubs such as sagebrush and shadscale	2
Heimsath et al. (2000)	Nunnock River, SE Australia	-36.605	149.493	40	0.74	86.9	Granodiorite	3	Laplacian of whole slope and erosion rate	2	Schlerophyll forest	3
Heimsath et al. (2005)	Nunnock River, SE Australia	-36.605	149.493	28	0.74	86.9	Granodiorite	3	Sediment flux from depth-integrated soil production rates and depth*gradient product	4	Schlerophyll forest	3
Hughes et al. (2009)	Charwell Basin, New Zealand	-42.450	173.357	88	1.42	116	Loess underlain by fluvial gravel terraces	1	Sediment flux from deposits and slope	4	Podocarp and beech forest	3
Hurst et al. (2012)	Feather River, CA, USA	39.652	-121.312	86	1.01	117	Granitoids	3	Best-fit *D* for 21 sites w/ridgetop Laplacians and cosmogenic-derived erosion rates	2	Mixed conifer forest	4
Hurst et al. (2013)	Feather River, CA, USA	39.724	-121.285	48 ± 18	1.10	113	Metavolcanics	3	Rdigetop Laplacian and erosion rates	2	Mixed conifer forest	4
Hurst et al. (2013)	Feather River, CA, USA	39.710	-121.262	88 ± 33	1.15	150	Granodiorite	3	Ridgetop Laplacian and erosion rates	2	Mixed conifer forest	4
Mattson and Bruhn (2001)	Lake Bonneville, UT, USA	40.48919	-112.32627	12 ± 3	0.41	43.7	Alluvial shoreline deposits	1	Scarp modeling	1	Scrubland with some trees	2
Mattson and Bruhn (2001)	Wasatch Fault Zone, UT, USA	40.72359	-111.82325	28 ± 11	0.42	49.1	Alluvial gravels	1	Scarp modeling	1	Scrubland with some trees	2

McGuire (2014).	San Francisco Volcanic Field in northern Arizona (SFVF)	35.390	-111.570	40	0.44	49.3	Basaltic cinder cones	1	Assumed initial shape and age in conjunction with a numerical model	3	Pinyon pine, sagebrush at lower elevation to Ponderosa pine forests at higher elevation	3
McGuire (2014).	Springerville Volcanic Field in east-central Arizona (SVF)	34.190	-109.570	50	0.50	56.4	Basaltic cinder cones	1	Assumed initial shape and age in conjunction with a numerical model	3	Ponderosa pine, Gambel oak, alligator bark juniper, Douglas fir, pinyon pine, sagebrush and juniper in lower elevations	3
McGuire (2014).	Medicine Lake Volcanic Field in northeastern California (MLVF)	41.640	-121.740	75	0.44	45.2	Basaltic and basaltic/andesitic cones	1	Assumed initial shape and age in conjunction with a numerical model	3	Lodgepole pine, ponderosa, Jeffrey pine, sugar pine, western white pine. Red and white fir at higher elevations. Western juniper at lower elevations	3
McKean et al. (1993)	East Bay Regional Park, CA, USA	37.974	-121.865	360 ± 55	0.34	43.1	Marine shale	2	Qs and slope	4	Grasslands	2
Nash (1980a)	Emmet County, MI, USA	45.575	-85.113	120	0.94	77.9	Cohesionless sand and gravel moraine deposits	1	Scarp modeling	1	Native hardwoods with scattered white pine and hemlocks, pine, oak, and beech	4
Nash (1980b)	Drum Mtns., UT, USA	39.650	-112.136	4	0.26	32.6	Alluvial gravels	1	Scarp modeling	1	Low shrubs such as sagebrush and shadscale	2
Nash (1984)	Hebgen Lake, MT, USA	44.701	-111.204	20 ± 2.4	0.72	62.2	Sand and gravel	1	Scarp modeling	1	Prairie grasses and some pine trees	3
Niviere and Marquis (2000)	Upper Rhine Graben, Germany	47.637	7.516	14	0.88	73	Fluvial gravels and coarse sands	1	Estimate from both scarp modeling and from estimating sediment volume at the toe of a man-made scarp.	1	Forested	4
Pelletier and Cline (2007)	Lathrop Wells, NV, USA	36.690	-116.510	39	0.07	10.9	Loose vesicular scoria lapilli	1	Numerical modeling using initial and current shape. Age of cone is 77 ka from radiometric dating	3	Mostly unvegetated	1
Pelletier et al. (2006)	Lake Bonneville, UT, USA	39.400	-113.700	10	0.20	25	Alluvial shoreline scarps (mostly sand and/or gravels)	1	Compared midpoint-slope-inverse method, slope-offset method, and full-scarp method	1	Grasses and shrubs	2

Pelletier et al. (2011)	Banco Bonito lava flow, Valles Caldera, NM, USA	36.840	-106.590	3-7 (4)	0.44	48.2	Rhyolite	3	Measured soil thickness and known age of lava flow to test a nonlinear, numerical LEM and choose the best parameter	3	Ponderosa pine, gamble oak scrublands, and mixed conifer forest	3
Perron et al. (2012)	Allegheny Plateau, PA, USA	39.971	-80.261	100 ± 8	0.98	105	Sandstone	2	Ridgetop Laplacian and erosion rate	2	Deciduous forest	4
Perron et al. (2012)	Gabilan Mesa, CA, USA	35.923	-120.826	124 ± 19	0.18	28.4	Poorly consolidated conglomerate	2	Ridgetop Laplacian and erosion rate	2	Grasses and oaks	3
Pierce and Colman (1986)	Big Lost River Valley, ID, USA	43.809	-113.336	~1-87 (21)	0.28	28.3	Carbonate gravels and sands	1	Scarp modeling of analytical solution with error function	1	South-facing slopes are shrub desert and the north-facing slopes are prairie grassland	2
Reneau (1988) reported in Heimsath et al. (2005)	Tennessee Valley, CA, USA	37.863	-122.550	50	0.94	94.2	Intensely sheared thrust sheets of greenstone, greywacke sandstone and chert (Franciscan assemblage)	2	Colluvial infilling of landslide deposits	4	Coastal grassland and scrub	2
Reneau (1988) reported in Heimsath et al. (2005)	Point Reyes, CA, USA	38.047	-122.852	30	0.93	99.1	Quartz diorite and granodiorite	3	Colluvial infilling of landslide deposits	4	Bishop pine forest	4
Reneau et al. (1989)	Clearwater River, WA, USA	47.660	-124.000	47	4.20	311	Silts, sandstones and conglomerates	2	Qs estimates from dating hollow deposits (~10,000 yr timescale) and slope.	4	Western hemlock and Pacific silver fir forest	5
Riggins et al. (2011)	Bodmin Moor, Cornwall, UK	50.508	-4.439	394 ± 163 (6)	1.96	114	Granite	3	Ridgetop Laplacian and soil production rate	2	Grasses, (previously hazel, and oak woodland)	4
Roering et al. (1999)	Sullivan Creek, OR, USA	43.463	-124.119	36 ± 16	2.00	168	Turbidite beds (Tyee Formation)	2	Minimized error between modeled erosion rates and measured erosion rates for non-linear erosion equation.	3	Douglas fir and mixed conifer forest	4
Roering et al. (2002)	Charwell River, South Island, New Zealand	-42.450	173.357	120 ± 80	1.42	116	5m thick loess cap on top of fluvial gravel terraces	1	Curvature and timescale of vegetation-driven creep (9K yr) on slope	2	Podocarp and beech forest	3

Roering et al. (2004)	Charwell River, South Island, New Zealand	-42.450	173.357	160 ± 50	1.42	116	Loess underlain by fluvial gravel terraces	1	Numerical modeling in a similar style to scarp diffusion (but assumes initial loess surface geometry instead)	3	Podocarp and beech forest	3
Rosenbloom and Anderson (1994)	Santa Cruz, CA, USA	36.984	-122.127	100	0.72	79.8	Mudstone	2	Numerical model with best-fit D	3	The lower terraces are farmed while the upper terraces are covered with grasslands. The lower terraces have never been forested.	2
Small et al. (1999)	Wind River Range, WY, USA	43.370	-109.750	176 ± 12 (2)	1.00	60.3	Granite and gneiss	3	Ridgetop Laplacian and erosion rates	2	Mostly unvegetated	6
Spelz et al. (2008)	Laguna Salada, Baja California, Mexico	32.075	-115.383	0.4 ± 0.3	0.04	8.3	Gravel terraces	1	Finite-slope and infinite-slope scarp modeling technique	1	Mostly unvegetated, but some vegetation near active fans and channel bars.	1
Tapponiier et al. (1990)	Qilian Shan, China	39.262	99.608	33 ± 17	0.11	11.9	Fanglomerates	1	Scarp modeling	1	Mostly unvegetated	1
This study	Great Smokey Mountains, NC, USA	35.622	-83.204	19 ± 1	1.38	154	Quartzite	3	Ridgetop Laplacian and erosion rates	2	Deciduous forest	4
This study	San Bernardino Mountains, CA, USA	34.051	-116.934	176 ± 21	0.59	72.9	Primarily granitic rocks (quartz monzonite and gneiss)	3	Ridgetop Laplacian and erosion rates	2	Chaparral and oak	3
This study	Wasatch Mountains, UT, USA	40.892	-111.865	83 ± 15	0.45	51.5	Gneiss	3	Ridgetop Laplacian and erosion rates	2	Patchy vegetation with trees, sage, and grasses	3
This study	San Gabriel Mountains, CA, USA	34.364	-117.992	71 ± 12	0.66	77.1	Primarily granitic and metamorphic rocks.	3	Ridgetop Laplacian and erosion rates	2	Chaparral, deciduous and conifers	3
This study	Tennessee Valley, CA, USA	37.850	-122.550	174 ± 21	0.89	84.4	Intensely sheared thrust sheets of greenstone, greywacke sandstone and chert (Franciscan assemblage)	2	Ridgetop Laplacian and erosion rates	2	Coastal grassland and scrub	2
This study	Oregon Coast Range, OR, USA	44.517	-123.844	167 ± 37	2.55	223	Tyee Sandstone	3	Ridgetop Laplacian and erosion rates	2	Dense coniferous forest	4

This study	Blasingame, CA, USA	36.954	-119.631	23 ± 3	0.26	38.7	Tonalite	3	Ridgetop Laplacian and erosion rate	2	Oak grassland	3
This study	Atacama Desert, Chile	-24.130	-69.990	1.4 ± 0.5	0.01	0.7	Granitic	3	Ridgetop Laplacian and erosion rates	2	Desert	1
This study	Atacama Desert, Chile	-29.770	-71.080	16 ± 2	0.07	7.8	Granitic	3	Ridgetop Laplacian and erosion rates	2	Desert	1
Walther et al. (2009)	Blue Mountains, WA, USA	46.148	-117.938	48 ± 7	0.82	74.4	Basalt bedrock, but blanketed with loess, which controls erosion rate.	2	Slope of line between differential erosion rate (from glass age estimate and peak profile of Mazama ash) and differential curvature.	2	Coniferous forest	4
West et al. (2014)[f]	Susquehanna Shale Hills Critical Observatory, PA, USA	40.667	-77.903	61 ± 33 (6)	0.95	97.6	Shale	2	Meteoric ^{10}Be and slope	4	Deciduous forest on hillslopes and hemlock and pine in valley	4

[a]If the exact location was not able to be identified, we used the location that best matched the site description. If multiple measurements were made for a region, we report the mean lat/lon for the study.

[b]Uncertainties are reported as they were presented in the original journals. If uncertainties were not reported, we calculated and reported the standard deviation of *D* and the number of estimates when possible. When a range is reported, we reported the value of *D* used in our analysis in parenthesis.

[c]Rock category: 1 = unconsolidated, 2 = sedimentary, 3 = Igneous/metamorphic.

[d]Technique category: 1 = Scarp modeling, 2 = Laplacian and erosion rates, 3 = LEM, 4 = Colluvial flux and slope, 5 = erosion rate and Laplacian.

[e]Vegetation category: 1 = Arid/desert, 2 = grasslands/scrublands, 3 = savannah/lightly forested, 4=forested.

[f]West et al. (2014) reported the range of *D* for noth-facing and south-facing slopes. We reported the mean of these values.

Table DR2

Site Location	Bedrock Erosion Rate (m/Myr)	Ridgetop Laplacian (x10^{-3} 1/m)	ρ_r/ρ_s	*D* (cm^2/yr)	Source of erosion rates	Source of topographic data
Great Smokey Mountains, NC, USA	27 ± 2	-28.2 ± 4.3	2	19 ± 1	Rate from Portenga and Bierman (2011). Rate originally determined by Matmon et al. (2003).	OpenTopo[a]

San Bernardino Mountains, CA, USA	1373 ± 148	-157.3 ± 7.3	2	175 ± 21	Rate from Willenbring et al. (2013). Rate originally determined by Binnie et al. (2007).	OpenTopo[a]
Wasatch Mountains, UT, USA	89 ± 9	-24.7 ± 0.6	2	83 ± 15	Rate from Willenbring et al. (2013). Rate originally determined by Stock et al. (2009).	OpenTopo[b]
San Gabriel Mountains, CA, USA	108 ± 17	-30.2 ± 0.6	2	71 ± 12	Rate from Willenbring et al. (2013). Rate originally determined by DiBiase et al. (2010)	OpenTopo[a]
Tennessee Valley, CA, USA	102 ± 23	-11.6 ± 1.4	2	174 ± 21	Rate from Portenga and Bierman (2011). Rate originally determined by Heimsath et al. (1997).	OpenTopo[a]
Oregon Coast Range, OR, USA	155 ± 30	-18.9 ± 2.4	2.27	206 ± 45	Rate from Portenga and Bierman (2011). Rate originally determined by Bierman et al. (2001).	OpenTopo[a]
Blasingame, CA, USA	30 ± 4	-26.9 ± 0.4	2	22 ± 3	Dixon et al. (2009)	OpenTopo[a]
Atacama Desert, Chile	1 ± 0	-24.6 ± 6.0.	3.25	1 ± 1	Owen et al. (2011)	J. Owen
Atacama Desert, Chile	27 ± 3	-29.1 ± 1.2	1.69	16 ± 2	Owen et al. (2011)	J. Owen

[a]Data downloaded from OpenTopography (http://opentopo.sdsc.edu). Lidar data acquisition and processing completed by the National Center for Airborne Laser Mapping (NCALM – http://www.ncalm.org). NCALM funding provided by NSF's Division of Earth Sciences, Instrumentation and Facilities Program.
[b]Data downloaded from OpenTopography (http://opentopo.sdsc.edu). Data collected by the State of Utah and its partners.

SUPPLEMENTAL REFERENCES

Almond, P.C., Roering, J.J., Hughes, M.W., Lutter, F.S., and Lebouteiller, C., 2008, Climatic and anthropogenic effects on soil transport rates and hillslope evolution: Sediment Dynamics in Changing Environments, v. Christchurch, New Zealand, p. 417–424.

Arrowsmith, J.R., Rhodes, D.D., and Pollard, D.D., 1998, Morphologic dating of scarps formed by repeated slip events along the San Andreas Fault, Carrizo Plain, California: Journal of Geophysical Research, v. 103, p. 10141–10160.

Avouac, J.P., 1993, Analysis of Scarp Profiles: Evaluation of Errors in Morphologic Dating: Journal of Geophysical Research, v. 98,

p. 6745, doi: 10.1029/92JB01962.

Avouac, J.P., and Peltzer, G., 1993, Active tectonics in southern Xinjiang, China: Analysis of terrace riser and normal fault scarp degradation along the Hotan-Qira Fault System: Journal of Geophysical Research: Solid Earth (1978–2012), v. 98, p. 21773–21807, doi: 10.1029/93JB02172.

Avouac, J.P., Tapponnier, P., Bai, M., You, H., and Wang, G., 1993, Active thrusting and folding along the northern Tien Shan and Late Cenozoic rotation of the Tarim relative to Dzungaria and Kazakhstan: Journal of Geophysical Research: Solid Earth (1978–2012), v. 98, p. 6755–6804, doi: 10.1029/92JB01963.

Begin, Z.B., 1992, Application of quantitative morphologic dating to paleo-seismicity of the northwestern Negev, Israel: Israel Journal of Earth Sciences, v. 41, p. 95–103.

Bierman, P.R., Clapp, E.M., Nichols, K.K., Gillespie, A.R., and Caffee, M.W., 2001, Using Cosmogenic Nuclide Measurements In Sediments To Understand Background Rates Of Erosion And Sediment Transport, *in* Harmon, R.S. and Doe, W.W. eds., Landscape Erosion and Evolution Modeling, New York, Springer US, p. 89–115, doi: 10.1007/978-1-4615-0575-4_5.

Binnie, S.A., Phillips, W.M., Summerfield, M.A., and Fifield, L.K., 2007, Tectonic uplift, threshold hillslopes, and denudation rates in a developing mountain range: Geology, v. 35, p. 743–5, doi: 10.1130/G23641A.1.

Bowman, D., and Gerson, R., 1986, Morphology of the latest Quaternary surface-faulting in the Gulf of Elat region, eastern Sinai: Tectonophysics, v. 128, p. 97–119, doi: 10.1016/0040-1951(86)90310-0.

Carretier, S., Ritz, J.F., Jackson, J., and Bayasgalan, A., 2002, Morphological dating of cumulative reverse fault scarps: examples from the Gurvan Bogd fault system, Mongolia: Geophysical Journal International, v. 148, p. 256–277.

Colman, S.M., and Watson, K., 1983, Ages estimated from a diffusion equation model for scarp degradation: Science, v. 221, p. 263–265, doi: 10.1126/science.221.4607.263.

DiBiase, R.A., Whipple, K.X., Heimsath, A.M., and Ouimet, W.B., 2010, Landscape form and millennial erosion rates in the San Gabriel Mountains, CA: Earth and Planetary Science Letters, v. 289, p. 134–144, doi: 10.1016/j.epsl.2009.10.036.

Dixon, J.L., Heimsath, A.M., Kaste, J., and Amundson, R., 2009, Climate-driven processes of hillslope weathering: Geology, v. 37, p. 975–978, doi: 10.1130/G30045A.1.

Enzel, Y., Amit, R., Porat, N., Zilberman, E., and Harrison, B.J., 1996, Estimating the ages of fault scarps in the Arava, Israel: Tectonophysics, v. 253, p. 305–317, doi: 10.1016/0040-1951(95)00072-0.

Fernandes, N.F., and Dietrich, W.E., 1997, Hillslope evolution by diffusive processes: The timescale for equilibrium adjustments: Water Resources Research, v. 33, p. 1307–1318.

Furbish, D.J., and Fagherazzi, S., 2001, Stability of creeping soil and implications for hillslope evolution: Water Resources Research, v. 37, p. 2607–2618.

Hanks, T.C., and Andrews, D.J., 1989, Effect of far-field slope on morphologic dating of scarplike landforms: Journal of Geophysical Research: Solid Earth (1978–2012), v. 94, p. 565–573, doi: 10.1029/JB094iB01p00565.

Hanks, T.C., and Wallace, R.E., 1985, Morphological analysis of the Lake Lahontan shoreline and Beachfront fault scarps, Pershing County, Nevada: Bulletin of the Seismological Society of America, v. 75, p. 835–846.

Hanks, T.C., Bucknam, R.C., Lajoie, K.R., and Wallace, R.E., 1984, Modification of wave-cut and faulting-controlled landforms: Journal of Geophysical Research, v. 89, p. 5771–5790.

Heimsath, A.M., Dietrich, W.E., Nishiizumi, K., and Finkel, R.C., 1997, The soil production function and landscape equilibrium: Nature, v. 388, p. 358–361.

Heimsath, A.M., E Dietrich, W., Nishiizumi, K., and Finkel, R.C., 1999, Cosmogenic nuclides, topography, and the spatial variation of soil depth: Geomorphology, v. 27, p. 151–172, doi: 10.1016/S0169-555X(98)00095-6.

Hurst, M.D., Mudd, S.M., Walcott, R., Attal, M., and Yoo, K., 2012, Using hilltop curvature to derive the spatial distribution of erosion rates: Journal of Geophysical Research, v. 117, p. F02017, doi: 10.1029/2011JF002057.

Matmon, A., Bierman, P.R., Larsen, J., Southworth, S., Pavich, M., Finkel, R.C., and Caffee, M.W., 2003, Erosion of an Ancient Mountain Range, The Great Smoky Mountains, North Carolina and Tennessee: v. 303, p. 817–855, doi: 10.2475/ajs.303.9.817.

Mattson, A., and Bruhn, R.L., 2001, Fault slip rates and initiation age based on diffusion equation modeling: Wasatch Fault Zone and eastern Great Basin: Journal of Geophysical Research: Solid Earth (1978–2012), v. 106, p. 13739–13750, doi: 10.1029/2001JB900003.

Nash, D., 1980a, Forms of bluffs degraded for different lengths of time in emmet county, Michigan, U.S.A.: Earth Surface Processes, v. 5, p. 331–345, doi: 10.1002/esp.3760050405.

Nash, D.B., 1980b, Morphologic dating of degraded normal fault scarps: The Journal of Geology, doi: 10.2307/30062456.

Nash, D.B., 1984, Morphologic dating of fluvial terrace scarps and fault scarps near West Yellowstone, Montana: Geological Society of America Bulletin, v. 95, p. 1413–1424, doi: 10.1130/0016-7606(1984)95<1413:MDOFTS>2.0.CO;2.

Niviere, B., and Marquis, G., 2000, Evolution of terrace risers along the upper Rhine graben inferred from morphologic dating methods: evidence of climatic and tectonic forcing: Geophysical Journal International, v. 141, p. 577–594, doi: 10.1046/j.1365-246x.2000.00123.x.

Pelletier, J.D., and Cline, M.L., 2007, Nonlinear slope-dependent sediment transport in cinder cone evolution: Geology,, doi: 10.1130/G23992A.1;2figures;DataRepositoryitem2007266.

Pelletier, J.D., McGuire, L.A., Ash, J.L., Engelder, T.M., Hill, L.E., Leroy, K.W., Orem, C.A., Rosenthal, W.S., Trees, M.A., Rasmussen, C., and Chorover, J., 2011, Calibration and testing of upland hillslope evolution models in a dated landscape: Banco Bonito, New Mexico: Journal of Geophysical Research, v. 116, p. F04004–24, doi: 10.1029/2011JF001976.

Perron, J.T., Kirchner, J.W., and Dietrich, W.E., 2009, Formation of evenly spaced ridges and valleys: Nature, v. 460, p. 502–505, doi: doi:10.1038/nature08174.

Petit, C., Gunnell, Y., Gonga-Saholiariliva, N., Meyer, B., and Séguinot, J., 2009, Faceted spurs at normal fault scarps: Insights from numerical modeling: Journal of Geophysical Research, v. 114, p. B05403–13, doi: 10.1029/2008JB005955.

Pierce, K.L., and Colman, S.M., 1986, Effect of height and orientation (microclimate) on geomorphic degradation rates and processes, late-glacial terrace scarps in central Idaho: Geological Society of America Bulletin, v. 97, p. 869–885, doi: 10.1130/0016-7606(1986)97<869:EOHAOM>2.0.CO;2.

Portenga, E.W., and Bierman, P.R., 2011, Understanding Earth's eroding surface with 10Be: GSA Today, v. 21, p. 4–10, doi: 10.1130/G111A.1.

Reneau, S.L., 1988, Depositional and erosional history of hollows: application to landslide location and frequency, long-term erosion rates, and the effects of climatic change [Ph.D. thesis]: Berkeley, University of California, 654 p.

Reneau, S.L., Dietrich, W.E., Rubin, M., Donahue, D.J., and Jull, A.J.T., 1989, Analysis of hillslope erosion rates using dated colluvial deposits: The Journal of Geology, v. 97, p. 45–63, doi: 10.2307/30062184.

Riggins, S.G., Anderson, R.S., Anderson, S.P., and Tye, A.M., 2011, Solving a conundrum of a steady-state hilltop with variable soil depths and production rates, Bodmin Moor, UK: Geomorphology, v. 128, p. 73–84, doi: 10.1016/j.geomorph.2010.12.023.

Roering, J.J., Almond, P., Tonkin, P., and McKean, J., 2002, Soil transport driven by biological processes over millennial time scales: Geology, v. 30, p. 1115–1118.

Roering, J.J., Kirchner, J.W., and Dietrich, W.E., 1999, Evidence for nonlinear, diffusive sediment transport on hillslopes and implications for landscape morphology: v. 35, p. 853–870, doi: 10.1029/1998WR900090.

Roering, J.J., Perron, J.T., and Kirchner, J.W., 2007, Functional relationships between denudation and hillslope form and relief: Earth and Planetary Science Letters, v. 264, p. 245–258.

Rosenbloom, N.A., and Anderson, R.S., 1994, Hillslope and channel evolution in a marine terraced landscape, Santa Cruz, California: Journal of Geophysical Research: Solid Earth (1978–2012), v. 99, p. 14013–14029, doi: 10.1029/94JB00048.

Small, E.E., Anderson, R.S., and Hancock, G.S., 1999, Estimates of the rate of regolith production using and from an alpine hillslope: Geomorphology, v. 27, p. 131–150, doi: 10.1016/S0169-555X(98)00094-4.

Spelz, R.M., Fletcher, J.M., Owen, L.A., and Caffee, M.W., 2008, Quaternary alluvial-fan development, climate and morphologic dating of fault scarps in Laguna Salada, Baja California, Mexico: Geomorphology, v. 102, p. 578–594, doi: 10.1016/j.geomorph.2008.06.001.

Stock, G.M., Frankel, K.L., Ehlers, T.A., Schaller, M., Briggs, S.M., and Finkel, R.C., 2009, Spatial and temporal variations in denudation of the Wasatch Mountains, Utah, USA: Lithosphere, v. 1, p. 34–40, doi: 10.1130/L15.1.

Tapponnier, P., Meyer, B., Avouac, J.P., Peltzer, G., Gaudemer, Y., Shunmin, G., Hongfa, X., Kelun, Y., Zhitai, C., Shuahua, C., and Huagang, D., 1990, Active thrusting and folding in the Qilian Shan, and decoupling between upper crust and mantle in northeastern Tibet: Earth and Planetary Science Letters, v. 97, p. 382–403, doi: 10.1016/0012-821X(90)90053-Z.

Walther, S.C., Roering, J.J., Almond, P.C., and Hughes, M.W., 2009, Long-term biogenic soil mixing and transport in a hilly, loess-mantled landscape: Blue Mountains of southeastern Washington: Catena, v. 79, p. 170–178, doi: 10.1016/j.catena.2009.08.003.

West, N., Kirby, E., Bierman, P., and Clarke, B.A., 2014, Aspect-dependent variations in regolith creep revealed by meteoric 10Be: Geology, v. 42, p. 507–510, doi: 10.1130/G35357.1.

Willenbring, J.K., Codilean, A.T., and McElroy, B., 2013, Earth is (mostly) flat: Apportionment of the flux of continental sediment over millennial time scales: Geology, v. 41, p. 343–346, doi: 10.1130/G33918.1.